RNA (2000), *6*:1142–1156. Cambridge University Press. Printed in the USA.

Substrate recognition by a eukaryotic RNase III: The double-stranded RNA-binding domain of Rnt1p selectively binds RNA containing a 5′-AGNN-3′ tetraloop

ROLAND NAGEL and MANUEL ARES, JR.

Center for the Molecular Biology of RNA, Sinsheimer Laboratories, University of California, Santa Cruz, Santa Cruz, California 95064, USA

ABSTRACT

Rnt1p is an RNase III homolog from budding yeast, required for processing snRNAs, snoRNAs, and rRNA. Numerous Rnt1p RNA substrates share potential to form a duplex structure with a terminal four-base loop with the sequence AGNN. Using a synthetic RNA modeled after the 25S rRNA 3′ ETS cleavage site we find that the AGNN loop is an important determinant of substrate selectivity. When this loop sequence is altered, the rate of Rnt1p cleavage is reduced. The reduction in cleavage rate can be attributed to reduced binding of the mutant substrate as measured by a gel-shift assay. Deletion of the nonconserved N-terminal domain of Rnt1p does not affect cleavage site choice or the ability of the enzyme to distinguish substrates that contain the AGNN loop, indicating that this region is not required for selective cleavage. Strikingly, a recombinant fragment of Rnt1p containing little more than the dsRBD is able to discriminate between wild-type and mutant loop sequences in a binding assay. We propose that a major determinant of AGNN loop recognition by Rnt1p is present in its dsRBD.

Keywords: dsRBD; pre-rRNA processing; endoribonuclease

INTRODUCTION

Every mature RNA is derived from a primary transcript by one or more RNA processing events. The many RNA processing events including cleavage, splicing, and modification are carried out by a diverse set of cellular factors. Some processing events are performed by relatively simple proteins such as nucleases, others by protein complexes like the exosome, others by small RNA–protein complexes like RNase P or snoRNPs, and still others by more complex RNPs like the spliceosome. In many cases these factors show exquisite specificity, altering only one or a few defined chemical bonds in a limited set of RNAs within the cell.

In yeast, the biogenesis of an eclectic set of RNAs including rRNA, snRNAs, and snoRNAs is enhanced by a member of the RNase III protein family called Rnt1p. Disruption of the *RNT1* gene has a devastating effect on cell growth, causing extreme temperature sensitivity (Abou Elela et al., 1996; Abou Elela & Ares, 1998; Chanfreau et al., 1998b). Initial studies of Rnt1p established its involvement in processing both 18S rRNA and 25S rRNA (Abou Elela et al., 1996). Recent results (Kufel et al., 1999) cast doubt on the interpretation that Rnt1p is directly required for 18S rRNA processing (Abou Elela et al., 1996) and instead suggest that the requirement of Rnt1p for 18S rRNA maturation is mediated indirectly through its role in snoRNA metabolism. For example Rnt1p is required for efficient accumulation of U14 (Chanfreau et al., 1998b) and U3 (C.-H. Ho, R. Nagel, H. Igel, & M. Ares, Jr., unpubl.) snoRNAs, which in turn are required for pre-18S rRNA cleavage events (Li et al., 1990; Hughes & Ares, 1991). In contrast, Rnt1p is directly required for maturation of yeast pre-25S rRNA through cleavage of a stem loop in the rRNA 3′ external transcribed spacer (3′ ETS) of the rRNA transcription unit (Abou Elela et al., 1996; Allmang & Tollervey, 1998; Kufel et al., 1999).

The involvement of Rnt1p in rRNA and ribosome metabolism must extend beyond rRNA cleavage events. Rnt1p is also required for the maturation of at least 20 snoRNAs from pre-snoRNA transcripts, some of which are polycistronic (Chanfreau et al., 1998a, 1998b; Qu et al., 1999). The snoRNAs that depend on Rnt1p in

Reprint requests to: Manuel Ares, Jr., Center for the Molecular Biology of RNA, Sinsheimer Laboratories, University of California, Santa Cruz, Santa Cruz, California 95064, USA; e-mail: ares@biology.ucsc.edu.

turn guide nearly half of the known position-specific 2′OCH3 and pseudouridylation modifications in rRNA (Samarsky & Fournier, 1999). The many levels at which Rnt1p contributes to the processing and modification of rRNA may explain much of the pleiotropic effects of *rnt1* mutations, and suggest that it may be difficult to dissect the specific contribution of the enzyme to any one step in the rRNA processing pathway.

Rnt1p cleaves synthetic duplex RNA lacking loops (Abou Elela et al., 1996), but many natural substrates are cleaved on both strands of an imperfect duplex region about 14–16 bp from a four-base loop sequence 5′-AGNN-3′ (Chanfreau et al., 1997, 1998a, 1998b; Abou Elela & Ares, 1998; Allmang et al., 1999; Kufel et al., 1999; Qu et al., 1999). Beyond comparisons of substrate structures there is little direct information concerning what RNA structures define an Rnt1p substrate. An Rnt1p site near the 3′ end of U2 snRNA is cleaved in vitro, even when the lower portion of the stem-loop structure on the 3′ side of the helix is deleted (Abou Elela & Ares, 1998). Cleavage can still take place on the truncated substrate at the correct position on the 5′ side of the helix, but this cleavage is lost when the 3′ side of the upper helix, but not the loop is removed (Abou Elela & Ares, 1998). This suggests that the 14–16-bp imperfect duplex and the four-base loop, but not the lower helix, are important components of Rnt1p substrate recognition. Recently the AGNN loop has been shown to contribute to substrate binding and positioning of the cleavage site (Chanfreau et al., 2000). Further experiments are necessary to determine how Rnt1p selects its substrates, however the presence of conserved sequences in bacterial RNase III or *Schizosaccharomyces pombe* pac1 substrates has not been observed (Rotondo et al., 1997; Nicholson, 1999; Zhou et al., 1999).

Comparison of Rnt1p protein structure with that of other RNAse III family members indicates that the yeast protein has a C-terminal double-stranded RNA binding domain (dsRBD) (St Johnston et al., 1992; Abou Elela et al., 1996; Rotondo & Frendewey, 1996). Immediately N-terminal to the dsRBD is a single copy of the "nuclease domain" characterized by a conserved pattern of carboxylate residues that may position metal ions in this magnesium-dependent enzyme (Abou Elela et al., 1996; Rotondo & Frendewey, 1996; Rotondo et al., 1997). Bacterial RNase III sequences do not extend much farther, but both *S. pombe* pac1 and *Saccharomyces cerevisiae* Rnt1p have long, nonconserved N-terminal domains of unknown function (Abou Elela et al., 1996; Rotondo & Frendewey, 1996). Recent experiments have suggested that this domain contributes to, but is not essential for dimerization (Lamontagne et al., 2000).

In this study, we have begun to dissect Rnt1p to determine how yeast RNAse III (Rnt1p) recognizes and cleaves its substrates, and which parts of the protein are required for function in vivo and in vitro. To answer these questions we have used different Rnt1 protein derivatives produced in bacteria and small substrate RNAs modeled after the 3′ ETS stem-loop. We establish that the presence of the 5′-AGNN-3′ loop enhances the rate of Rnt1p cleavage. This enhanced cleavage rate is likely due to enhanced substrate binding, as shown by a gel-shift assay, and is consistent with data using a different substrate (Chanfreau et al., 2000). Deletion of the N-terminal domain does not alter the preference of the enzyme for cleavage of the AGNN-loop-containing substrate, indicating that it is unlikely this region of the protein contributes elements necessary for identifying the loop. However the isolated Rnt1p dsRBD preferentially binds AGNN-loop-containing substrate. This indicates that the dsRBDs of the Rnt1p dimer contribute to substrate selection through recognition of the AGNN loop. We propose that the Rnt1p dsRBD contains unique elements that confer sequence or structure-specific recognition of the AGNN RNA loop, in addition to elements necessary for binding dsRNA.

RESULTS

A small RNA derived from the rRNA 3′ ETS is accurately cleaved in vitro

To understand how Rnt1p interacts with its substrates, we designed and tested a model RNA based on the natural rRNA 3′ ETS processing site. Initial studies indicated that Rnt1p cleaved the 3′ ETS once at position +20 relative to the mature end of the 3′ end of 25S ribosomal RNA in a nearly 1-kb-long transcript containing a large segment of 25S rRNA (Abou Elela et al., 1996). The difficulty in handling this large substrate motivated the development of a shorter model substrate that is a 65-nt sequence derived from the 3′ ETS stem loop (WT) (Fig. 1C). Primer extension of the WT substrate maps cleavage to positions +15 and +14 on the 5′ side of the stem loop (Fig. 1A). With a separate primer, cleavage on the 3′ side of the loop maps to between positions +50 and +49, relative to the mature 3′ end of 25S ribosomal RNA (Fig. 1B), and not at +20 as reported previously (Abou Elela et al., 1996). The difference between these results and those reported previously could be due to heterogeneity in substrate folding or problems related to the activity of the enzyme, and we do not currently understand the basis for this discrepancy. None of the preparations of the enzyme we now routinely produce cleave the model substrate at position +20.

The Rnt1p cleavage sites observed using the model 3′ ETS substrate in vitro (Fig. 1C) are similar to those mapped in vivo (Kufel et al., 1999). In vitro cleavage appears to occur predominantly after position +15 rather than at +14 on the 5′ side of the stem-loop, and at +50 more so than at +49 as observed in vivo (Kufel et al.,

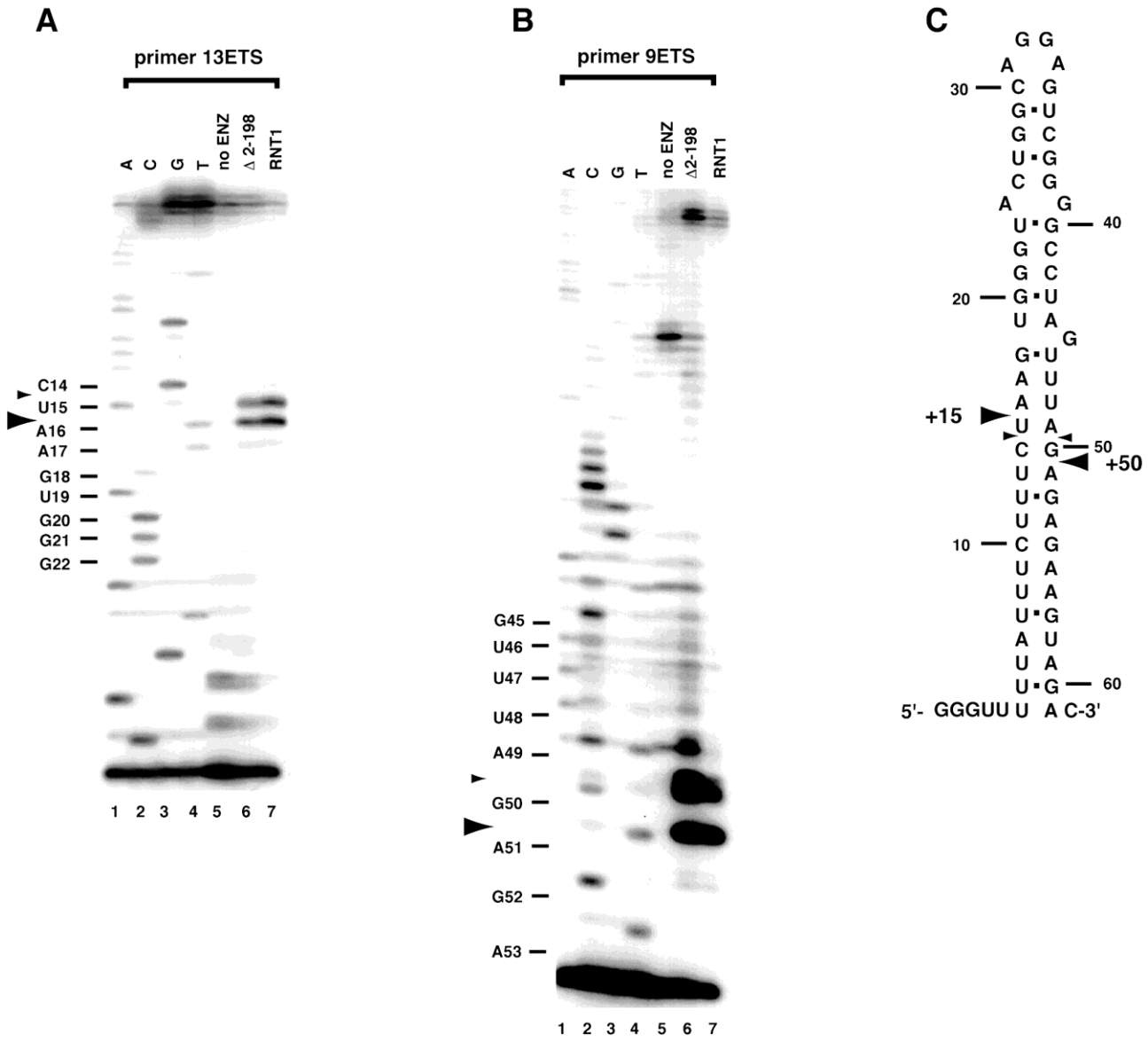

FIGURE 1. In vitro mapping of Rnt1p cleavage sites in the model 3′ ETS RNA substrate. **A**: Primer extension using primer 13ETS. Lanes 1, 2, 3, and 4 are sequencing reactions in which ddA, ddC, ddG, and ddT have been added. Also shown are RNA cleavage reactions with no added enzyme (lane 5), RNT1Δ2–198 (lane 6), and Rnt1p (lane 7). Sequence at the major primer extension termination is shown to the left of the panel and arrows indicate positions of termination products. **B**: Same as for **A** except that primer 9ETS was used. **C**: Positions of cleavage of the 65-nt 3′ ETS model substrate. Vertical arrows indicate the terminal 3′ nucleotide of primers 9ETS and 13ETS. Horizontal black arrows indicate in vitro cleavage sites observed for both RNT1Δ2–198 and the full-length Rnt1p enzyme. The small arrows also represent the in vivo cleavage sites (Kufel et al., 1999).

1999; see Fig. 1C). One possible reason for this discrepancy could be that detection of the upstream of the two sites by primer extension can occur only on RNA that is only cut once, and such partially cut products may not be normal reaction intermediates. It is also possible that the bacterially produced enzyme behaves slightly differently than the native enzyme. Despite these differences, the model RNA should allow accurate in vitro assessment of the function of Rnt1p at the 3′ ETS cleavage site.

The upper helix, but not the lower helix, is essential for Rnt1p cleavage at the upstream site

Cleavage of the Rnt1p site in the U2 3′ flank occurs in the absence of the 3′ strand of the lower helix (Abou Elela & Ares, 1998). To determine whether this is also true for 3′ ETS cleavage, we produced a set of 5′-end-labeled WT RNA molecules that differ sequentially by a single nucleotide, using mild base treatment of WT RNA

(Fig. 2A, lane 2). This 5′-end-labeled, partially hydrolyzed pool of RNA was challenged with Rnt1p to define the 3′ limit of the minimal substrate. WT RNAs extending beyond A49 are cleaved, as they disappear after incubation with Rnt1p (Fig. 2A, lanes 3 and 4). In contrast, base-hydrolyzed substrate molecules that terminate at positions 5′ of A49 are resistant to Rnt1p cleavage, indicating that efficiently cleaved substrates must extend at least to position 50. A control reaction shows that cleavage of the same amount of untreated RNA was complete by 30 s (Fig. 2A, lanes 5–7). We conclude that significant determinants for cleavage reside in the double-stranded region to the loop side of the cleavage sites (the upper helix). Although it is possible the lower helix could form through annealing of short RNA segments, the substrate has been denatured and the incubation with Rnt1p is brief, so that it is unlikely that the lower helix is present in substrates that have been base hydrolyzed at positions just beyond +50. Cleavage of these RNAs is efficient, arguing that the lower helix is not essential, consistent with results using truncated U2 3′ end substrates (Abou Elela & Ares, 1998). It appears the lower helix makes some contribution to the rate of cleavage however, because substrates that extend past G50 have increasing cleavage efficiencies as estimated by their rates of disappearance (Fig. 2A). One explanation for the difference between the requirements for the upper and lower segments might be that a helix carrying an AGNN loop could be bound more efficiently by the enzyme (Chan-

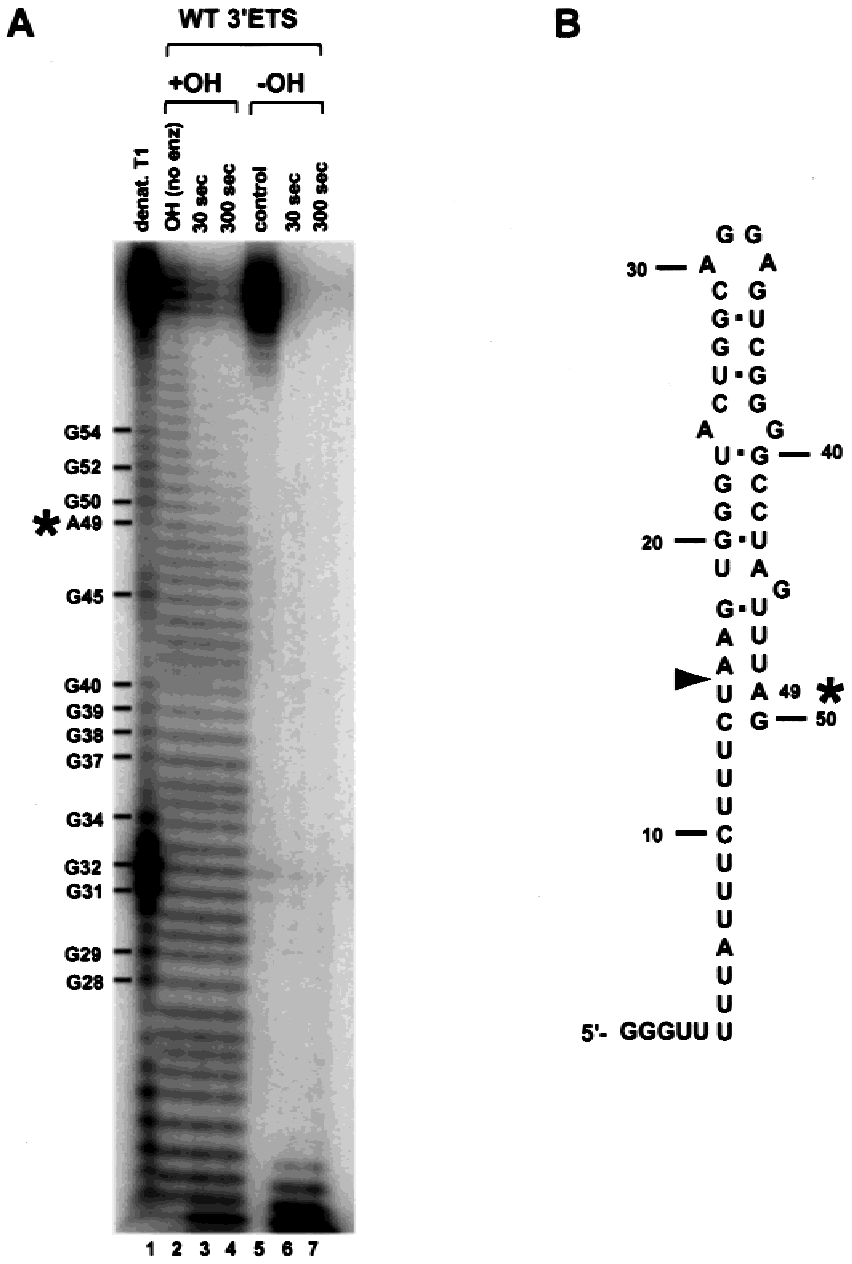

FIGURE 2. Delimitation of the 3′ border of an Rnt1p substrate. **A:** Rnt1p cleavage of WT 3′ ETS substrate treated with hydroxide ion (+OH, lanes 2–4) or control, no hydroxide treatment (−OH, lanes 5–7). Lane 1: T1 nuclease G track sequencing; lane 2: hydroxide-ion-treated substrate (no added enzyme); lanes 3 and 4: Rnt1p cleavage products of hydroxide-ion-treated substrate at 30 s (lane 3) or 300 s (lane 4); lane 5: 5′-end-labeled WT RNA substrate (no added enzyme); lanes 6 and 7: Rnt1p cleavage of control substrate at 30 s (lane 6) and at 300 s (lane 7). **B**: Model of the minimal 3′ ETS substrate. Arrowhead indicates normal cleavage site on the 5′ side of the stem loop at +15 and ∗ denotes the largest WT RNA substrate for which no Rnt1p cleavage is observed on the 5′ side of the stem loop.

freau et al., 2000; see below). To test this idea we examined the effect of the AGNN loop on the rate of cleavage by Rnt1p.

Rate of Rnt1p cleavage is influenced by the AGNN loop

Although Rnt1p cleaves synthetic perfect duplex substrates (Abou Elela et al., 1996), many natural Rnt1p substrates are imperfect RNA stems with a loop that has the consensus sequence AGNN (Chanfreau et al., 1998b, 2000). We asked whether or not the loop was important for Rnt1p cleavage rates (Fig. 3). We produced a mutant (GU) of the wild-type (WT) 3′ ETS substrate in which the AGNN loop is replaced with GUGA (Fig. 3C). This sequence is a member of the GNRA class of tetraloops that form a stable characteristic structure (for review, see Jucker & Pardi, 1995). We tested the cleavage rate of WT and GU substrates at different concentrations of KCl. At 50 mM KCl, cleavage of both substrates occurs, as shown by the appearance of the product P1, although the rate of cleavage of the mutant substrate is lower (Fig. 3A, lanes 1–3, compare to lanes 4–6). At 100 mM KCl cleavage of the WT substrate is not greatly reduced (Fig. 3A, lanes 7–9), however cleavage of the mutant substrate GU is affected (Fig. 3A, lanes 10–12). At 200 mM KCl a further reduction of WT cleavage rate is observed (Fig. 3A, lanes 13–15), and cleavage of the GU substrate is not observed (Fig. 3A, lanes 16–18). We conclude that Rnt1p cleavage rates are enhanced by the presence of an AGNN loop found on many of its natural substrates.

To exclude the possibility that the loop mutation destroys the double-stranded character of the model substrate, we probed for differences between the structures of WT and GU RNA. We treated the WT and GU substrate RNAs with limiting concentrations of T1 nuclease at 100 mM KCl (Fig. 3B), conditions under which Rnt1p selectively cleaves the WT substrate (Fig. 3A, lanes 7–12). As a reference, the same RNAs were treated with T1 under denaturing conditions to map G residues (Fig. 3B, lanes 1 and 6). Under nondenaturing conditions, only G31 and G32 of the WT RNA are significantly cleaved (Fig. 3B, lanes 2–5), whereas other G residues are well protected from T1. Because G31 and G32 reside within the AGNN loop, and G residues between positions 18 and 40 are protected from T1, we

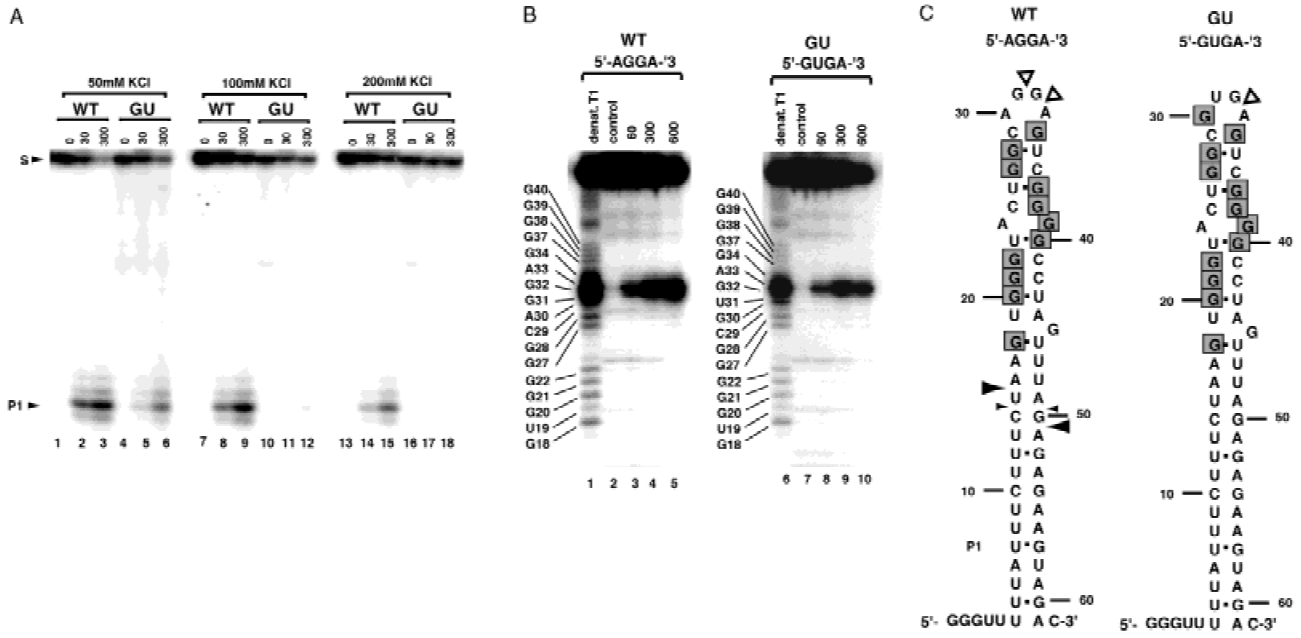

FIGURE 3. Cleavage of model WT and GU mutant 3′ ETS RNA. **A**: Cleavage reaction time courses using wild-type (WT) and mutant (GU) 3′ ETS substrate RNAs at various KCl concentrations. Reactions were sampled at 0, 30 and 300 s. Lanes 1–3: 50 mM KCl using WT RNA; lanes 4–6: 50 mM KCl and GU RNA; lanes 7–9: 100 mM KCl and WT RNA; lanes 10–12: 100 mM KCl and GU RNA; lanes 13–15: 200 mM KCl and WT RNA; lanes 16–18: 200 mM KCl and GU RNA. S: input substrate; P1: 18 nt 5′ cleavage product. **B:** Nuclease T1 probing of WT and GU RNA. Denaturing 20% acrylamide gel is shown. WT or GU sequence generated with T1 under denaturing conditions is indicated to the left of lanes 1–5 or 6–10, respectively. Lane 1: T1 digestion using denaturing conditions; lane 2: no added enzyme; lanes 3–5: time course of T1 digestion of WT RNA under native conditions at 60 s (lane 3); 300 s (lane 4); and 600 s (lane 5). Lanes 6–10 are identical except that GU mutant 3′ ETS RNA was used. **C**: Secondary structure models for WT RNA (5′-AGGA-3′ loop) and GU RNA (5′-GUGA-3′ loop). Positions cleaved by T1 nuclease are shown using open arrowheads. Positions protected from T1 nuclease digestion are indicated by gray squares. Sequence numbering is relative to the mature 3′ end of 25S ribosomal RNA.

conclude that the WT 3′ ETS substrate structure is close to that predicted (Abou Elela et al., 1996; Fig. 3C). Digestion of the GU mutant RNA shows that only G32 is accessible to T1 (Fig. 3B, lanes 7–10), consistent with the formation of a G-A base pair within the tetraloop (Jucker & Pardi, 1995) that would lead to decreased accessibility of G30. The other G residues in the GU substrate are protected from T1 to similar extents as in the WT substrate (Fig. 3B, compare lanes 7–10 with lanes 2–5), consistent with the interpretation that the loop mutation causes little if any disruption of the duplex segments of the substrate. Although subtle perturbations not detectable by T1 could affect cleavage of the GU mutant substrate, we conclude that both WT and GU 3′ ETS RNA differ primarily in their loops. Because they are present in many natural substrates (Chanfreau et al., 1998a, 2000), and because Rnt1p cleavage rate is higher on substrates that contain them (Fig. 3B), it seems likely that the AGNN loop is an important determinant of substrate selection.

Higher relative cleavage rates are due in part to higher Rnt1p affinity for AGNN-loop-containing substrates

One reason for different cleavage rates of the two substrates might be that Rnt1p binds the GU substrate less tightly than the WT substrate. We assayed the ability of Rnt1p to retard the migration of either the WT (AGNN loop) or GU (GNRA loop) substrates in a native-gel assay (Fig. 4). We estimated the apparent dissociation constant (K_d) in the gel at 4 °C after incubation in the absence of Mg^{2+} (to prevent cleavage of the substrate) and under ionic conditions (100 mM KCl) in which cleavage rate experiments (Fig. 3B) indicate that the enzyme discriminates between the substrates. We find that the enzyme has an apparent K_d of 10–12 nM for the WT substrate but that the K_d for the GU mutant substrate is greater than 36 nM. This analysis suggests that Rnt1p has at least a fourfold greater affinity for the AGNN-loop-containing substrate than for the mutant, and that this difference could explain the increased cleavage rate on the WT substrate relative to the mutant (Fig. 3B). Using a different substrate and a different binding assay, Chanfreau et al. (2000) recently found a similar change in the relative K_d upon mutation of the loop. Thus the AGNN-loop-containing substrate may be cleaved at a higher rate (Fig. 3B) simply because it is bound more tightly to the enzyme (Fig. 4).

The N-terminal domain of Rnt1p is not required for dimerization, cleavage, cleavage site selection, or discrimination of the AGNN loop

Because bacterial RNase III is a dimer (see Nicholson, 1999), it is important to know for certain whether the yeast protein is dimeric or might have another

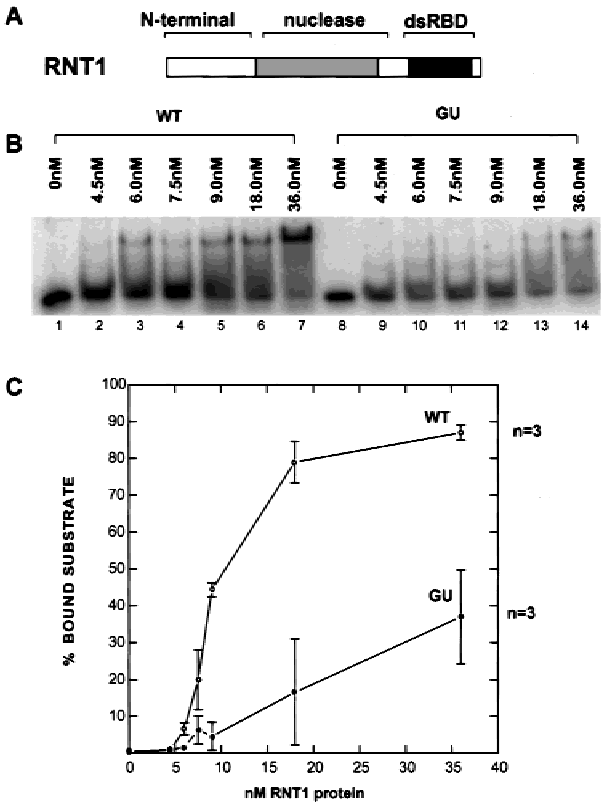

FIGURE 4. Full-length Rnt1p selectively binds the AGNN-loop-containing substrate. **A:** Domains of Rnt1p. The white box is the N-terminal domain; the gray box is the region of sequence homology with the RNAse III nuclease domain; and the black box is the region of sequence homology with dsRBDs. **B:** RNA mobility-shift assay. In vitro-transcribed RNA representing WT or GU RNA (see Fig. 3C) incubated with increasing concentrations of full-length Rnt1p and run on a nondenaturing gel. Lanes 1–7 and 8–14 contain 0 nM, 4.5 nM, 6.0 nM, 7.5 nM, 9.0 nM, 18 nM, and 36 nM full-length Rnt1p. **C**: Graph of percent of substrate bound *versus* full-length Rnt1p protein concentration. Plot shows binding curves for WT substrate (open circles) and GU substrate (filled circles). Each point is the mean of three separate determinations ($n = 3$) and the standard error is shown.

quaternary structure, possibly owing to the extended N-terminal domain (Abou Elela et al., 1996; Rotondo & Frendewey, 1996; see Fig. 5A). To address this, the sedimentation behavior of bacterially expressed Rnt1p in sucrose gradients was compared with that of marker protein complexes with known molecular mass. A Coomassie-stained gel of such a gradient is shown in Figure 5B. Migration of bovine serum albumin (BSA, 68-kDa monomer, peaking in fraction 4), aldolase (158-kDa tetramer, peaking in fraction 6), and catalase (232-kDa tetramer, peaking in fraction 10) are indicated. Rnt1p peaks in fraction 5 between the BSA and aldolase markers. Because the Rnt1p polypeptide chain is calculated to be 55 kDa in mass, the migration of the native protein is most consistent with a homodimer of 110 kDa. Evidence from gel exclusion columns that Rnt1p is a dimer include a description of tetramers and other higher-order complexes (Lamontagne et al., 2000); however under our conditions the full length protein behaves uniformly (Fig. 5B).

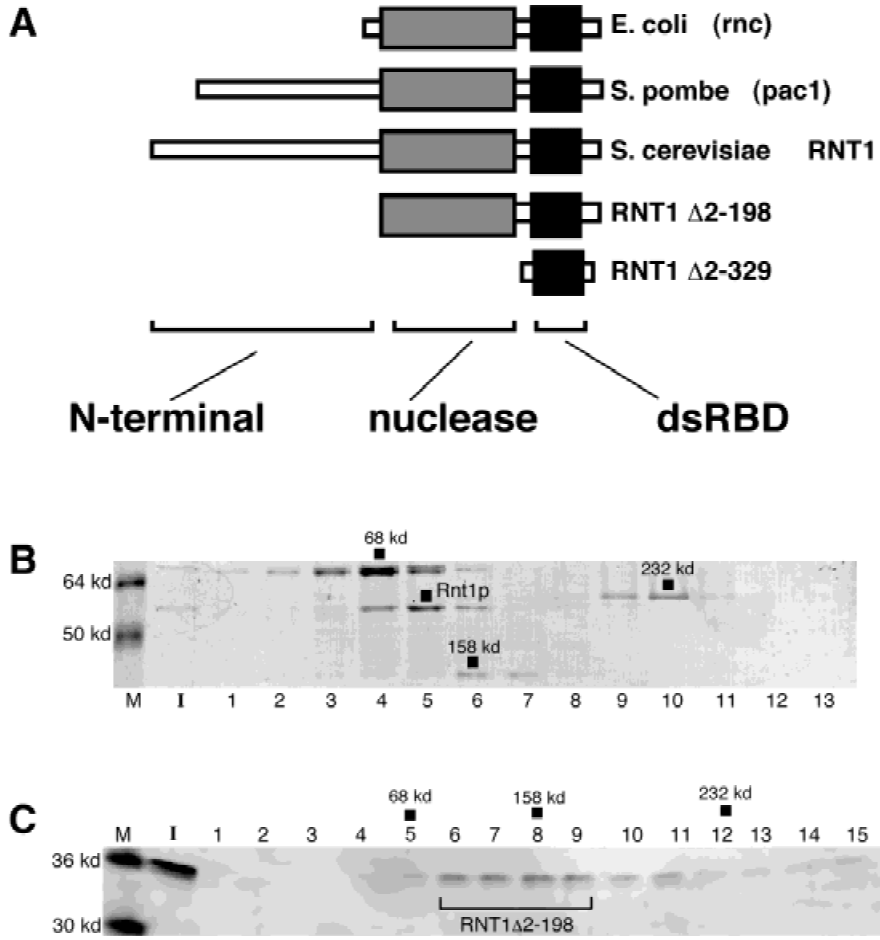

FIGURE 5. The N-terminal domain of Rnt1p is not required for dimerization, cleavage, or cleavage site selection. **A**: Alignment of RNAse III family members from *E. coli* (rnc), *S. pombe* (pac1), and *S. cerevisiae* (RNT1) showing similarity of domain structures consistent with a double-stranded RNA-binding domain (dsRBD, black box), nuclease domain (gray box), and a nonconserved N-terminal domain. Recombinant versions of Rnt1p used in this study in addition to the full-length version are RNT1Δ2–198 (N-terminal deletion), and RNT1Δ2–329 (containing little more than the dsRBD). **B**: Coomassie staining of an SDS polyacrylamide gel of fractions from a sucrose-density gradient. Molecular weight standards are shown in the left lane in kilodaltons. I: input sample of RNT1Δ2–198 protein. Lanes 1–13 each contain a 25-μL sample from each of 13 gradient fractions, numbered from top of the gradient to the bottom. Fractions containing peak concentrations of marker proteins and the position of Rnt1p are indicated with black squares. **C**: Western analysis of sucrose gradient containing RNT1Δ2–198 protein. Lanes 1–15 each contain 25 μL from each of 15 fractions that were resolved on an SDS PAGE gel, transferred to nitrocellulose, and probed using rabbit serum containing Rnt1p antibodies (see Materials and methods). Fractions containing peak concentrations of marker proteins are indicated with black squares. Fractions containing peak concentration of RNT1Δ2-198 protein are indicated with a square bracket.

To begin determining what features of Rnt1p allow it to cleave selectively substrates containing the AGNN loop, we evaluated the importance of the nonconserved N-terminal domain (Figs. 5C and 6). The extended N-terminal domains of *S. cerevisiae* Rnt1p and *S. pombe* pac1 are not highly related to each other or to metazoan members of the RNase III protein family, nor are they found in bacterial RNase III (Abou Elela et al., 1996; Rotondo & Frendewey, 1996; see Fig. 5A). To assess the function of this domain we prepared an N-terminally deleted version of Rnt1p (RNT1Δ2–198) and compared its behavior to that of full-length Rnt1p. A previous study concluded that the N-terminal domain contributes to, but is not required for dimerization, and suggested that a detectable fraction of an Rnt1p derivative lacking the N-terminal domain was monomeric (Lamontagne et al., 2000). Because the oligomeric state of the enzyme could be important to the means by which it recognizes its substrate, we examined the sedimentation behavior of a similar Rnt1p derivative lacking the N-terminal domain (RNT1Δ2–198) under conditions in which full-length Rnt1p can discriminate AGNN-loop-containing substrates (Fig. 5C). To discourage aggregation and precipitation, which we have found to be problematic with N-terminally deleted derivatives of Rnt1p, we used western blots and an antibody against Rnt1p to detect small amounts of soluble RNT1Δ2–198 in the gradient fractions (Fig. 5C). Under these condi-

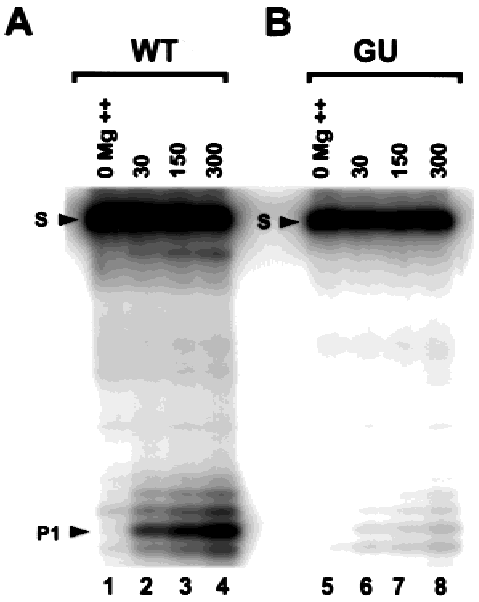

FIGURE 6. Cleavage of WT or GU RNA by RNT1Δ2–198. **A**: WT RNA. Lane 1: no added $MgCl_2$; lane 2: 30 s; lane 3: 150 s; lane 4: 300 s. S is the 65-nt model substrate; P1 is the 18-nt 5′ cleavage product. **B**: GU RNA. Lane 5: no added $MgCl_2$; lane 6: 30 s; lane 7: 150 s; lane 8: 300 s.

tions, RNT1Δ2–198 migrates primarily as a dimer, with very little if any protein migrating as a monomer. The trailing of RNT1Δ2–198 into the heavier fractions of the gradient is consistent with a tendency of the truncated protein to form multimers or to aggregate, and is not seen with the full-length protein at higher protein concentrations (Fig. 5B). Because RNT1Δ2–198 migrates predominantly as a dimer on sucrose gradients, we conclude that the N-terminal domain is not required for dimerization under conditions in which the AGNN loop substrates are selectively bound and cleaved by the wild-type protein.

To determine whether the N-terminal domain is necessary for RNA-cleavage-site selection, we assayed the sucrose gradient fractions in Figure 5C using a 3′ ETS substrate (data not shown). Cleavage activity peaks in the same fractions as those containing RNT1Δ2–198 (Fig. 5C, lanes 6–9) indicating that the dimeric and higher-order forms of the protein are active. Cleavage sites used are identical to those observed for the full-length Rnt1p (Fig. 1A). Therefore, like full-length Rnt1p, RNT1Δ2–198 accurately cleaves the 3′ ETS in vitro.

Because of the solubility problems noted above, it is difficult to measure with any confidence the cleavage efficiency of RNT1Δ2–198 as compared to full-length Rnt1p under different salt and temperature conditions. However, because it displays the same cleavage site specificity as the full-length enzyme, we were able to ask whether the N-terminally deleted RNT1Δ2–198 protein can discriminate AGNN-loop-containing substrates. To do this we evaluated the rate of cleavage of WT (AGNN loop) and GU (GNRA loop) RNAs under reaction conditions (100 mM KCl) that allow full-length Rnt1p to discriminate between them. The WT substrate is cleaved at a greater rate (Fig. 6, lanes 1–4) than the GU substrate (Fig. 6, lanes 5–8). We conclude that the N-terminal domain of Rnt1p is dispensable for discrimination of AGNN-loop-containing substrates. This conclusion suggests that the special elements of Rnt1p that allow preferential cleavage of AGNN-loop-containing substrates lie elsewhere in the protein.

A fragment of Rnt1p containing the dsRBD selectively binds the AGNN-loop-containing substrate

One possible mechanism by which full-length Rnt1p might bind selectively to AGNN-loop-containing substrates would be through its dsRBD. In this view, the Rnt1p dsRBD would have both a general affinity for dsRNA and additional affinity for dsRNA adjacent to an AGNN loop. A recent NMR study of the staufen dsRBD indicates one way in which a dsRBD may interact with an RNA loop (Ramos et al., 2000). To test whether the Rnt1p dsRBD preferentially binds dsRNA with an AGNN loop, we prepared a recombinant fragment spanning the dsRBD (RNT1Δ2–329, Fig. 7A), and evaluated binding to WT and GU RNA using a mobility shift assay (Fig. 7B,C). The results show that RNT1Δ2–329 preferentially binds the WT substrate as compared to the GU mutant substrate. RNT1Δ2–329 binds the WT substrate with an apparent K_d of approximately 750 nM (Fig. 7B, lanes 1–7). In comparison, RNT1Δ2–329 binds poorly to the mutant GU loop substrate with an apparent K_d slightly less than 5 μM (Fig. 7B, lanes 8–14; 7C). Although the absolute affinity of the isolated dsRBD for the substrate RNA is down about two orders of magnitude compared to that observed with the complete protein (Fig. 4), the relative affinity of the proteins for the two substrates is similar. Affinity of the isolated dsRBD for the mutant substrate is not absent, and is about fourfold less than for the substrate with the AGNN loop. The lower absolute affinity is expected, as presumably the complete protein contains other elements that may enhance substrate binding. On the other hand, the similar relative affinities may be hinting that the dsRBD contains all the Rnt1p elements involved in loop discrimination. We conclude that RNT1Δ2–329 carries important determinants of Rnt1p substrate binding that permit identification of AGNN loops.

Both the N-terminal domain and the dsRBD are necessary for function in vivo

Studies presented above show that the N-terminal domain is unnecessary for cleavage site selection or AGNN loop discrimination, and suggest that the Rnt1p dsRBDs are important for substrate selection through

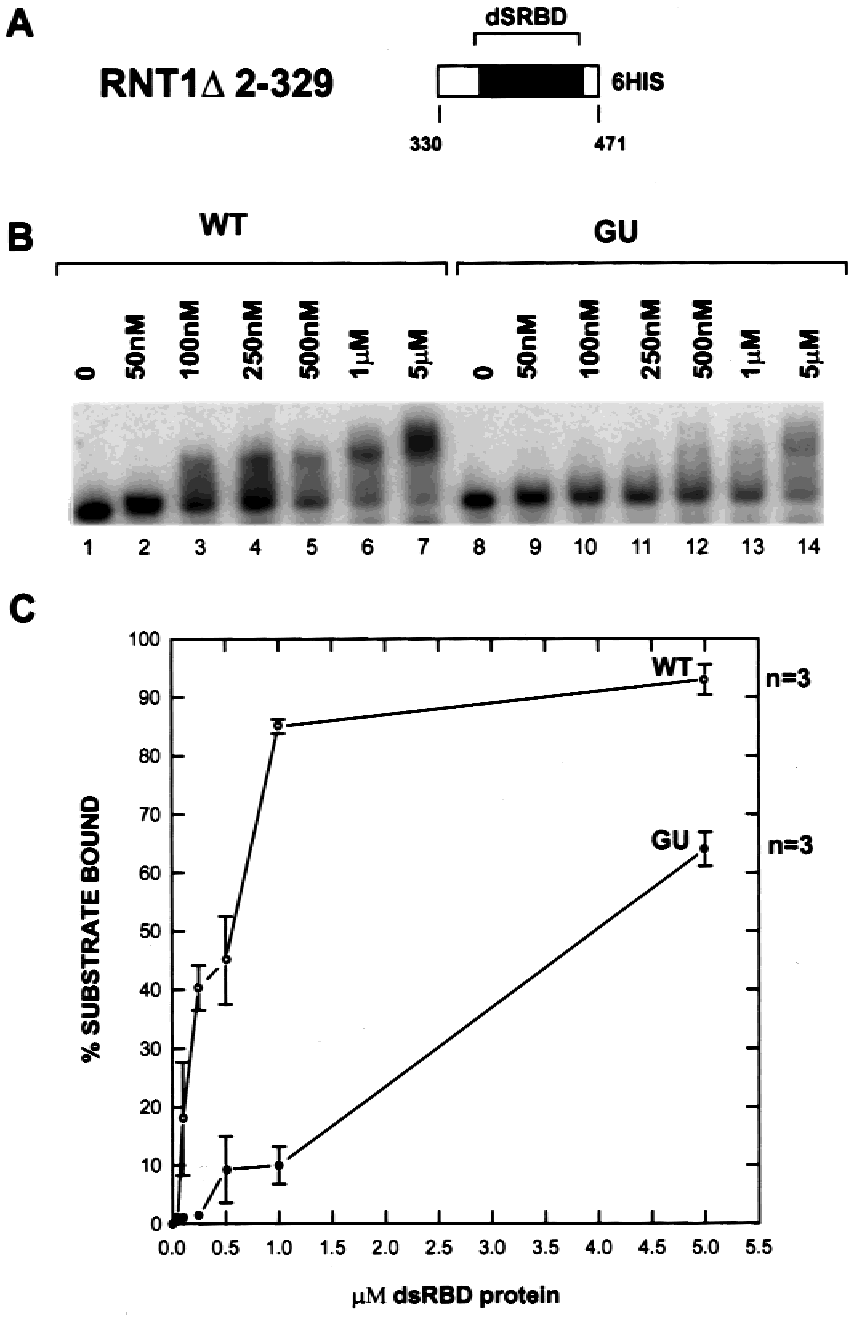

FIGURE 7. The Rnt1p dsRBD selectively binds the AGNN-loop-containing substrate. **A**: Diagram of RNT1Δ2–329, which contains the dsRBD of Rnt1p (residues 330–471). The black box indicates the region of sequence homology with dsRBDs. **B**: RNA mobility-shift assay. In vitro-transcribed RNA representing WT or GU RNA (see Fig. 3C) incubated with increasing concentrations of RNT1Δ2–329 and run on a nondenaturing gel. Lanes 1–7 and 8–14 contain 0 nM, 50 nM, 100 nM, 250 nM, 500 nM, 1 μM, and 5 μM protein. **C**: Graph of percent substrate bound *versus* protein concentration. Plots show binding curves for WT substrate (open circles) and GU substrate (filled circles). Each point is the mean of three separate determinations ($n = 3$) and the standard error is shown.

binding interactions with the conserved AGNN RNA loop. To test the functional significance of these parts of the protein in vivo, we made mutant alleles of *RNT1* (Fig. 8A) and tested their ability to support growth of the *rnt::HIS3* disruption strain (Fig. 8B), and correct processing of the 3′ end of 25S rRNA, using an RNAse protection assay (Fig. 8C). As a control for N-terminal deletions, the wild-type *RNT1* gene was modified to contain an *Nde*I site at its start codon (*RNT1*-Nde, Fig. 8A). This mutation does not produce a detectable growth defect, even at 37° (Fig. 8B; data not shown), but does lead to slight inhibition of the 25S rRNA 3′-end processing. This mild loss of activity is indicated in our assay by the increase in the level of the 80–90 nt extensions on the 3′ end of 25S rRNA (Fig. 8C, compare lane 3 with lane 2). Complete inactivation or loss

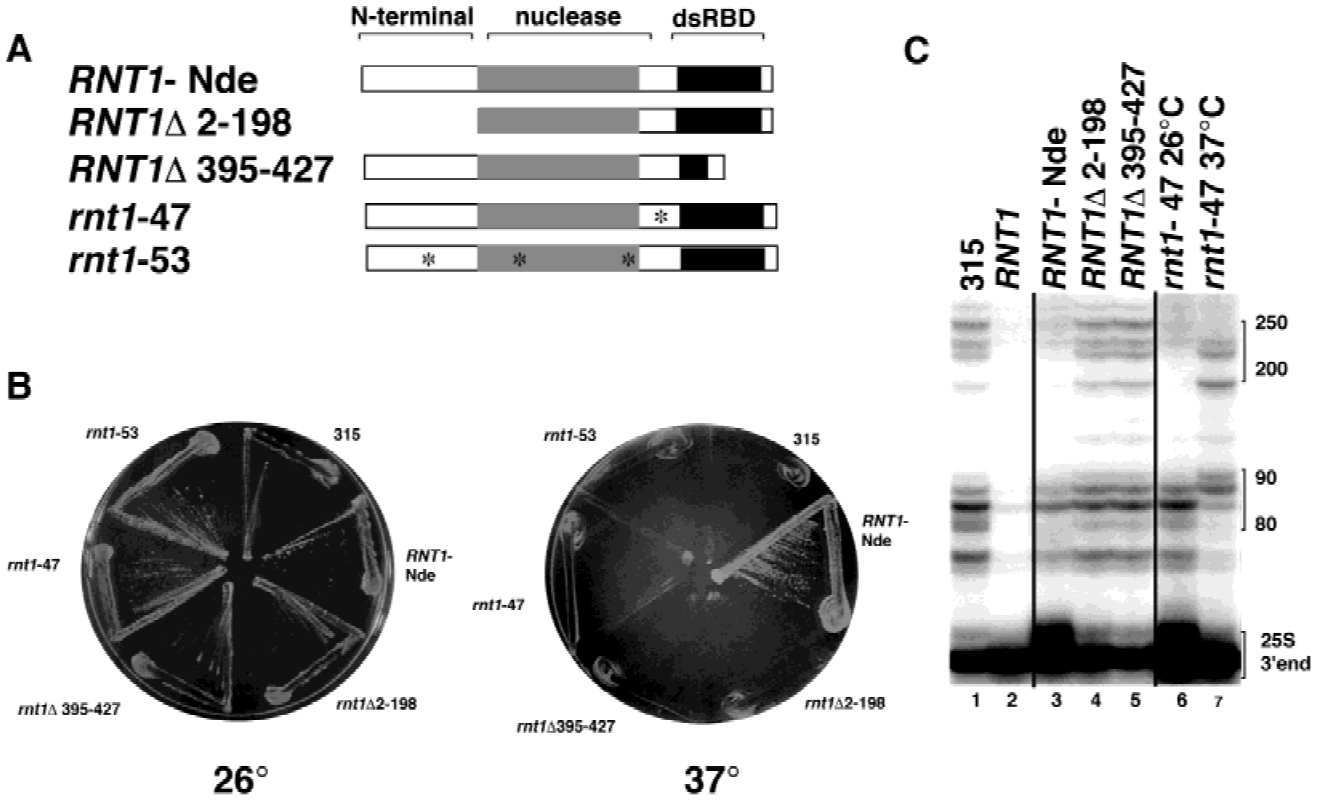

FIGURE 8. In vivo analysis of *RNT1* function. **A**: The *RNT1* gene from *S. cerevisiae*, including its native promoter and terminator regions, was cloned in pRS315. *RNT1*-Nde contains an *NdeI* site at the start codon; RNT1Δ2–198 lacks the N-terminal domain (see also Fig. 5); RNT1Δ395–427 lacks a segment of the dsRBD; *rnt1*-47 contains a point mutation changing I338 to T; *rnt1*-53 contains three substitutions (see Materials and methods). **B**: Complementation of the *rnt1::HIS3* disruption by *RNT1* alleles described in **A** incubated at 26 °C or 37 °C for 2 days. **C**: Maturation of 25S rRNA in strains carrying different *RNT1* alleles. Lanes 1–7 are as indicated; extended 25S rRNAs are indicated on the right of the panel; the signal derived from correctly processed 25S rRNA is indicated.

of Rnt1p results in the accumulation of longer 3′ extended forms of the 25S rRNA and a reduction in mature 25S rRNA (Abou Elela et al., 1996; Allmang & Tollervey, 1998; Kufel et al., 1999; Lamontagne et al., 2000; Fig. 8C, lane 1).

Expression of *RNT1*Δ2–198 in vivo does not rescue the growth defect of the *rnt::HIS3* strain at 26 °C or 36 °C (Fig. 8B), and does not prevent accumulation of both the 80–90 nt and the 200–250 nt 3′ extended forms of 25S rRNA, or the reduction in 25S rRNA levels (Fig. 8C, lane 4). Therefore cells expressing only *RNT1*Δ2–198 are defective in 3′ ETS processing, consistent with the absence of *RNT1* function. We conclude that, although it is not essential for enzyme activity, the N-terminal domain of the Rnt1p is important for function in vivo. The observation that a similar construct seems functional when over-expressed as a two-hybrid fusion protein (Lamontagne et al., 2000) suggests this is simply due to the need for a nuclear localization signal. An allele of *RNT1* lacking a segment coding for the dsRBD (*RNT1*Δ395–427) cannot complement the *rnt1::HIS3* growth defect (Fig. 8B), and does not prevent the accumulation of extended forms of the 3′ ETS rRNA (Fig. 8C, lane 5). This shows that the dsRBD of Rnt1p is important for its activity in vivo.

To identify functional regions of Rnt1p that might not be apparent from phylogenetic comparisons, we looked for temperature-sensitive alleles of *RNT1*. Two alleles, *rnt1*-47 and *rnt1*-53, were found in a screen for temperature sensitivity after mutagenesis of plasmid sequences by PCR. The *rnt1*-47 allele contains a single-point mutation changing isoleucine 338 to threonine in the region between the nuclease domain and the conserved sequences of the dsRBD. The *rnt1*-53 allele contains mutations that lead to three amino acid substitutions, one in the N-terminal domain, and two in the nuclease domain, one of which is in the highly conserved RNAse III signature sequence (Rotondo et al., 1995). As expected by their behavior in the original screen, these alleles complement the *rnt1::HIS3* disruption at permissive temperature, but not at restrictive temperature (Fig. 8B). Analysis of RNA from *rnt1*-47 reveals a slight accumulation of 3′ ETS RNA at 26 °C, indicating that *rnt1*-47 is mildly compromised at permissive temperature. A shift to nonpermissive temperature results in much greater accumulation of the more

3′ extended 25S RNAs, and reduction of mature 25S rRNA characteristic of more severe loss of *RNT1* function (Fig. 8C, compare lanes 6 and 7). Thus a single I-to-T substitution between the nuclease domain and the dsRBD can reduce the function of Rnt1p in vivo, especially at increased temperatures.

DISCUSSION

We are seeking to understand how *S. cerevisiae* RNAse III Rnt1p processes a diverse class of RNAs. Using a model substrate patterned after the rRNA 3′ ETS cleavage site (Fig. 1) we show that the AGNN loop found on many natural Rnt1p substrates contributes to the rate of cleavage by Rnt1p (Fig. 3). The increased cleavage rate may be due to the greater affinity of the enzyme for the loop-containing substrate (Fig. 4; see also Chanfreau et al., 2000). This effect of RNA loop identity on cleavage rates has not been observed in bacterial RNase III. Like bacterial RNase III, the yeast enzyme is a dimer (Fig. 5; see also Lamontagne et al., 2000). The N-terminal domain that distinguishes Rnt1p from the bacterial enzymes is not required for dimerization (Fig. 5; see also Lamontagne et al., 2000), RNA cleavage, or cleavage site selection (Fig. 6; see also Lamontagne et al., 2000). Significantly this domain is unnecessary for identification of the AGNN loop (Fig. 6), indicating that AGNN loop-discrimination elements are elsewhere in the protein. Consistent with this, we show that a segment of Rnt1p containing little more than the dsRBD selectively binds the AGNN-loop-containing substrate (Fig. 7) with about the same relative K_d as the complete protein (Fig. 4). This suggests that Rnt1p selectively cleaves dsRNA near an AGNN loop because its dsRBDs selectively recognize the AGNN loop sequence or structure.

How do dsRBDs mediate site-specific RNA binding?

The findings described above have implications for the action of other proteins that contain dsRBDs. Numerous bacterial RNase III proteins have been studied, and, although substrate recognition elements differ (for example, see Conrad et al., 1998; Nicholson, 1999), neither these nor any of the *S. pombe* pac1 substrate RNAs have an obvious feature resembling the AGNN loop of Rnt1p substrates. Study of *Escherichia coli* RNase III has revealed evidence for selection by antideterminants (Zhang & Nicholson, 1997), whereby the presence of certain sequences restricts binding and cleavage, and their absence identifies the substrate. A similar effect of loop size and position has been hypothesized to restrict sites of modification by ADARs, enzymes that promiscuously modify adenosines to inosines in perfect duplex RNA, but display high selectivity on natural substrates and model substrates with engineered loops (Lehmann & Bass, 1999).

Given the positive effect that the AGNN loop has on binding of the isolated dsRBD of Rnt1p (Fig. 7), there may be several ways in which dsRBDs promote site-specific binding to natural imperfect duplexes such as RNase III, ADAR, or other substrates. One way would be negative, whereby compatible segments of duplex are identified by their length or the absence of interfering elements, as suggested for *E. coli* RNase III (Zhang & Nicholson, 1997) and ADAR1 (Lehmann & Bass, 1999). The other is positive, whereby specific sequence or structural elements in terminal (or internal) loops interact positively with the dsRBD, as appears to be the case for Rnt1p and the AGNN loop (Figs. 3, 4, 6, and 7). The imperfect base pairing in the upper helix of the 3′ ETS substrate contributes negatively to binding, as replacing the G-U and G-A base pairs with G-C improves binding (V. Juan, D. Sussman, R. Nagel, M. Ares, Jr, and C. Wilson, unpubl.). Thus the natural substrates are likely composed of both negative elements and positive elements as may befit the need for efficient binding and rapid turnover of the enzyme. It remains to be seen whether internal AGNN loops can enhance Rnt1p dsRBD binding.

As the Rnt1p dsRBD can recognize AGNN loops (Fig. 7), which elements of the dsRBD carry the determinants of AGNN loop recognition? A recent NMR structure of a staufen dsRBD complexed with a dsRNA containing a four-base loop reveals interactions with the first alpha helix (α1) of the dsRBD (Ramos et al., 2000). The amino acids in this region vary in different dsRBDs and could carry determinants of RNA sequence-specific binding (Ramos et al., 2000). In this view, residues of α1 of at least one of the Rnt1p dsRBDs would be positioned near the AGNN loop. The Rnt1p dsRBD is unusual in that it does not have the conserved GxxH motif found in loop 2 of the staufen, XlbpA, and *E. coli* RNase III dsRBDs. Loop 2 residues interact with the minor groove in the two solved dsRBD–dsRNA complexes, but the precise interactions are different in the different complexes (Ryter & Schultz, 1998; Ramos et al., 2000). Residues corresponding to loop 2 of the Rnt1p dsRBD do not align well with classical dsRBDs and thus are candidates for determinants of AGNN loop binding. In this view, the dsRBD would be oriented in the opposite direction relative to the loop from that found in the staufen complex (Ramos et al., 2000), with loop 2 of the dsRBD interacting with the AGNN loop. Additional experiments will be necessary to determine precisely which elements of the Rnt1p dsRBD account for AGNN loop selectivity.

A model for Rnt1p substrate recognition: Interaction between at least one dsRBD and the AGNN loop is important for both substrate selectivity and cleavage site selection

Based on several observations, we propose the following model for Rnt1p substrate selectivity and cleavage

site selection. Rnt1p can cleave dsRNA not containing AGNN loops by virtue of its association with dsRNA regions through interactions mediated by the dsRBDs (Abou Elela et al., 1996). This means that although many known natural substrates carry the AGNN loop (Chanfreau et al., 1998a, 2000), there may be natural substrates that do not carry the loop. Substrate selectivity occurs because segments of dsRNA that end with an AGNN loop are preferentially bound by Rnt1p through additional interactions between the loop and at least one of the two dsRBDs in the dimeric protein. In the simplest model, one dsRBD is associated with the AGNN loop-adjacent dsRNA segment (the upper helix) through both its general dsRNA-binding activity and additional contacts with the loop, whereas the other dsRBD is associated with the lower helix through its general dsRNA-binding activity. If this is true, the interaction with the lower helix is likely to be dispensable, as the lower helix is not essential (Abou Elela & Ares, 1998; Fig. 2), and does not seem to be a consistent feature of all natural Rnt1p substrates.

Adding or subtracting base pairs in the duplex region between the loop and the cleavage sites causes the cleavage sites to move relative to the local sequence, such that they are positioned a fixed distance from the loop (Chanfreau et al., 2000). The finding that AGNN loop recognition is in part mediated by the dsRBD (Fig. 7) suggests that the dsRBD helps position the cleavage site by measuring the distance from the loop. In one of the solved structures, the dsRBD spans the equivalent of approximately 16 bp of duplex RNA (Ryter & Schultz, 1998). In the other structure, the dsRBD binds partly to the minor groove face of a four-base loop and partly to a 12-bp segment of perfect duplex (Ramos et al., 2000). Interestingly, the distance between the AGNN loop and the cleavage sites in many Rnt1p substrates is 14–16 bp (Chanfreau et al., 1997, 1998a, 1998b; Abou Elela & Ares, 1998; Allmang et al., 1999; Kufel et al., 1999; Qu et al., 1999; Seipelt et al., 1999). Whether the Rnt1p dsRBD binds to the loop itself, as in the staufen structure, or to the nearby dsRNA, access of the RNA by the nuclease domain could be restricted by the position of the dsRBD relative to the RNA loop. It is not necessary to invoke any special measuring function to the dsRBD for this model. Rather, structural constraints that normally position the nuclease active sites relative to the dsRBDs in the Rnt1p dimer could fix the active sites relative to the loop. Thus the dsRBD likely has two important roles: increasing affinity and selectivity of the enzyme for the AGNN-loop-containing substrate during the initial binding events, and identifying the cleavage sites by measuring the distance between the loop and the nuclease active sites. This predicts that substrates that do not contain the AGNN loop may be cleaved more readily at multiple sites within a duplex region, provided that other features of the duplex do not additionally restrict binding as discussed above.

Coordinate cleavage of an asymmetric substrate by a homodimeric enzyme

In many experiments, including those shown in Figures 1, 3, and 6, we and others (Abou Elela et al., 1996; Chanfreau et al., 1997, 1998a, 1998b; Abou Elela & Ares, 1998; Allmang et al., 1999; Seipelt et al., 1999) have observed that bacterially produced Rnt1p cleaves most substrate RNAs in a coordinate fashion. Coordinate cleavage is loosely defined as the situation that leads to the following observations. The products of complete Rnt1p digestion suffer two cuts relative to the initial substrate. During the reaction time course, once-cut substrate molecules appear with similar kinetics as products, and do not accumulate prior to formation of complete products, nor disappear as the reaction progresses, as would be expected if once-cut molecules were intermediates in the reaction pathway. Such once-cut molecules are not abundant and do not behave as kinetic intermediates in the in vitro reactions with many different Rnt1p substrates. Either the enzyme binds once-cut substrates far more avidly than uncut substrate or the two cleavage events occur after a single binding event, with the enzyme only rarely dissociating from the RNA after cutting only once.

Because we find that molecules 3′ truncated at or near the natural downstream cleavage site are poor substrates (Fig. 2), we favor the second possibility. Since the protein is a dimer (Fig. 5), it contains two dsRBDs. As there is only one AGNN loop in the substrate, the enzyme–substrate complex must be asymmetrical. We suggest that one dsRBD is associated with the loop and the upper helix, and the other with the lower helix, as the lower helix contributes to cleavage efficiency even though it is not essential (Abou Elela & Ares, 1998; Fig. 2). This hypothesis can be tested if heterodimeric Rnt1p derivatives can be constructed that carry mutations in the dsRBD or nuclease domains that render the enzyme complex partly active.

Surprisingly, cleavage in vivo seems not to be coordinate, as Rnt1p-processed RNA products that accumulate in a *rat1-1* strain are evenly distributed between those cut at the upstream site and those cut at the downstream site (Allmang et al., 1999; Kufel et al., 1999). Furthermore, processing in cell extracts, even those from stains lacking Rnt1p and to which recombinant Rnt1p has been added back, show far less coordinate cleavage than reactions with the purified protein (Chanfreau et al., 1997; Seipelt et al., 1999). This suggests that some as yet unidentified factor may dissociate Rnt1p from its RNA substrate after only a single cleavage event has occurred. Such a factor could aid in ensuring that Rnt1p-processed RNA molecules, all of

which require further processing by other enzymes, are efficiently hastened along their processing pathways.

MATERIALS AND METHODS

Deoxyoligonucleotides

Oligonucleotides were synthesized by Cruachem, and were gel purified before use. Oligonucleotides used for primer extension, PCR, and mutagenesis were:

9ETS: 5′-GTCTACTTC-3′;
13ETS: 5′-CCCCGACTCCTGC-3′;
(1): 5′-AAGCTTTTCCCCCAAACATATGGGCTCAAAA-3′;
(2): 5′-CCTTAACAAGCGGCCGCGCTTGTATCTGAGAATTTT-3′;
(3): 5′-AAGCATATGCCTCCAAAATTACCAGAG-3′;
(4): 5′-AAGCCGTATACCATGGATCCAAGGAATAATTTGCCC-3′;
3′ ETSAGGA: 5′-GTCTACTTCTCTCTAAACTAGGCCCCGACTCCTGCCAGTACCCACTTAGAAAGAAATAAAAACCCTATAGTGAGTCGTATTA-3′;
3′ ETSGUGA: 5′-GTCTACTTCTCTCTAAACTAGGCCCCGACACACGCCAGTACCCACTTAGAAAGAAATAAAAACCCTATAGTGAGTCGTATTA-3′;
T7 17mer: 5′-TAATACGACTCACTATA-3′.

Protein expression and purification

Protein expression constructs for *E. coli* were cloned using the T7 RNA polymerase expression vectors pET24b and pET21d and the *E. coli* host expression strain BL21(DE3). A series of C-terminally 6HIS-tagged versions of Rnt1p were constructed. A Vent polymerase PCR fragment generated by primers (1) and (2) using pRS315-*RNT1* as template was cut with *Nde*I and *Not*I and subcloned into pET24b digested with *Nde*I and *Not*I. The resulting plasmid pL-RNTx6HIS encodes full-length Rnt1p fused to six histidines. A Vent polymerase PCR fragment generated using primers (2) and (3) was cut using *Nde*I and *Not*I and subcloned into pET24b cut with *Nde*I and *Not*I. The resulting clone pΔ2–198 encodes a protein that lacks residues 2–198 of Rnt1p and contains a C-terminal 6HIS tag. A Vent polymerase PCR fragment generated using primers (4) and (2) was cut with *Nco*I and *Not*I and cloned into pET21d that had been linearized using *Nco*I and *Not*I. This plasmid, pΔ2–329, encodes a protein that lacks residues 2–329 of Rnt1p and contains C-terminal 6HIS tag. This construct represents the isolated Rnt1p dsRBD. All derivatives have the amino acid sequence AAALGHHHHHH appended to the C-terminal serine S471 of the native Rnt1p sequence.

All derivatives of Rnt1p were expressed in BL21(DE3) (Studier et al., 1990) and purified to greater that 90% homogeneity by affinity chromatography with nickel (II) nitriloacetic acid agarose. Protein preparations were dialyzed into RNT1 Storage Buffer (30 mM Tris-HCl, pH 7.9, 100 mM KCl, and 50% glycerol, 0.1 mM EDTA, 0.1 mM DTT), stored at −20 °C. Proteins were diluted in RNT1 dilution buffer containing 30 mM Tris-HCl, 0.1 mM EDTA, 0.1 mM DTT, and 50% glycerol.

Primer extension

Primer-extension reactions were conducted as described previously (Nagel et al., 1998) with the following modifications. Unlabeled WT RNA (0.1 pmol) was cleaved in a Rnt1p cleavage reaction (described above). Rnt1p cleavage fragments were purified by phenol/chloroform extraction. Cleavage fragments were resuspended in 5 μL of water and 2.5 μL extended with either 0.1 pmol of ^{32}P-5′-end-labeled primer 9ETS or 13ETS. Primers were annealed by heating to 90 °C for 1 min then cooled to 30 ° for 30 min. Extension reactions were incubated at 30 °C for 60 min, phenol/chloroform extracted and ethanol precipitated. 3′ ETS RNA substrate (0.25 pmol) was used in sequencing reactions that contained ddNTP terminator concentration of 200 uM in each reaction.

Rnt1p enzyme assays

Model 3′ ETS RNA transcripts were prepared using T7 RNA polymerase using oligonucleotides as templates as described previously (Milligan & Uhlenbeck, 1989). T7 transcripts were treated with calf intestinal phosphatase (CIP; Boehringer Mannheim) to remove 5′ triphosphate, and were 5′-end-labeled with T4 polynucleotide kinase (New England Biolabs) using [γ-^{32}P]-ATP. End-labeled transcripts were purified by gel electrophoresis, cut from the gel, and eluted overnight in RNA Elution Buffer (0.5 M ammonium acetate, 0.1 mM EDTA, and 0.1% SDS). RNA was phenol/chloroform extracted, ethanol precipitated, and resuspended in TE buffer at a concentration of 1 μM.

Rnt1p was incubated with substrate RNAs in 10 μL of 30 mM Tris-HCl, pH 8.0, 100 fmol of labeled RNA substrate, KCl as required, and 2.0 fmol of Rnt1p prepared by 1:5000 dilution of 1 mg/mL Rnt1p in RNT1 dilution buffer (30 mM Tris-HCL, pH 8.0, and 50% glycerol). Reactions were conducted at 30 °C, initiated by addition of $MgCl_2$, and stopped by the addition of EDTA and formamide dye mix for gel electrophoresis. Cleavage reactions using RNT1Δ2–198 were identical except 6.4 fmol of RNT1Δ2–198 was used and prepared by 1:10 dilution of a 0.05-mg/mL stock of RNT1Δ2–198 protein in RNT1 dilution buffer. Product amounts were determined by quantitation using a Molecular Dynamics PhosphorImager.

Structure probing

Gel-purified substrate RNA was heated to 95 °C for 1 min and snap cooled on ice. T1 nuclease digestions were essentially as described (Bevilacqua et al., 1998) with the following modifications. G track sequencing reactions were prepared by T1 nuclease digestion under denaturing conditions. Briefly 2 μL (0.2 pmol) of 5′-end-labeled RNA was added to 3 μL of 9 M urea and heated to 90 °C with the cap off the tube for 2 min, reducing the volume to 3 μL. Then, 2 μL of 0.05 U/μL T1 nuclease was added and the mixture was incubated at 30 °C for 20 min. The reaction was quenched by the addition of 2 μL of 1 μg/μL tRNA, and 20 μL of TE buffer, phenol/chloroform extracted, and ethanol precipitated. Reactions were dissolved in formamide dye and loaded onto 20% denaturing polyacrylamide gels. Hydroxide ladders were prepared by addition of 1 μL of 0.01 M NaOH and 1 μL of tRNA in TE

(10 mM Tris-HCl, 1 mM EDTA, pH 8.0) to 1 μL (0.1 pmol) of labeled substrate RNA in TE. Reactions were heated to 65 °C for 10 min, neutralized by the addition of 3 μL of 3 M sodium acetate and 1 μL of 1 μg/μL of *E. coli* tRNA, ethanol precipitated and resuspended in 4 μL of TE. Native structure T1 mapping reactions contained 2 μL of substrate RNA (0.2 pmol), 1 μL of 1 μg/μL *E. coli* tRNA, and 1 μL of 0.01 U/μL T1 nuclease in TE. The reaction was incubated at 30 °C, and 1-μL aliquots of the reactions were removed at 1, 5, and 10 min and mixed with 1 μL formamide dye mix before loading onto 20% denaturing acrylamide gels.

Binding assays

Binding for full-length Rnt1p and derivatives was determined by native-gel mobility-shift assays. Binding reactions were done in a final volume of 10 μL containing 30 mM Tris-HCl, pH 8.0, 100 mM KCl, 0.25 mM EDTA, 1 μL of trace amounts of WT or GU RNA and 1 μL of Rnt1p. Reactions were initiated by the addition of 1 μL of an appropriate dilution of Rnt1p in RNT1 dilution buffer (30 mM Tris-HCl, pH 8.0, and 50% glycerol) and incubated at 25 °C for 5 min. Binding reactions were then placed on ice and 1 μL of a 50% glycerol containing 0.05% xylene cyanol loading dye was added. Binding studies using the full-length Rnt1p were resolved using 3.5% acrylamide (30:1 acrylamide/bis)/0.5% agarose gels containing 5% glycerol and 0.5× TBE prepared using the following protocol. Thirty-five milliliters of 7% acrylamide were made by adding 8.16 mL of 30% acrylamide, 7 mL of 50% glycerol, and 19.84 mL of water and heating briefly in a microwave oven for 15 s. Thirty-five milliliters of 1% agarose in 1 × TBE at 55 °C were added to the warmed acrylamide mixture. One hundred microliters of 20% ammonium persulfate and 100 μL of TEMED were added and the gel mixture was poured without delay and allowed to set at room temperature for 30 min before placing at 4 ° C for 60 min. Gels were pre-run at 4 °C for 30 min at 85 V before samples were loaded. Samples were run at 85 V for 120 min. Binding of the RNT1Δ2–329 dsRBD was tested using identical binding reactions as described above except that bound RNA complexes were resolved from free RNA using 4.5% (80:1 acrylamide/bis) native gels in a 0.5 × TBE buffer system. All gels were dried and exposed to Molecular Dynamics PhosphorImager screen for autoradiography and quantification.

Sucrose gradient centrifugation

Bacterially expressed Rnt1p and RNT1Δ2–198 proteins were analyzed on 5–20% sucrose gradients as follows. Gradients were constructed in 4 mL tubes using 2 mL of 5% sucrose, 30 mM Tris-HCl, pH 7.9, 100 mM KCl, and 2 mL of 20% sucrose, 30 mM Tris-HCl, 100 mM KCl, and stored at 4 °C. A 10-μL sample of enzyme at a concentration of 1 mg/mL in 30 mM Tris-HCl, 100 mM KCl was mixed with a 10-μL sample of marker protein mix. Marker protein mix contained 1.0 mg/mL BSA (68 kDa), 1.0 mg/mL rabbit aldolase (158 kDa), and 1.0 mg/mL catalase (262 kDa). Marker proteins were from Pharmacia. The mixture was applied to gradients and centrifuged in an SW60Ti rotor (Beckman) at 38,000 rpm for 16 h at 4 °C. Fractions were collected from the bottom of the gradient and were numbered in reverse order of their collection.

Preparation of polyclonal Rnt1p antibodies

Recombinant Rnt1p was prepared as described previously and subjected to preparative electrophoresis through 12% SDS PAGE gels. The Rnt1p band was identified by staining with 0.5% Coomassie blue in water for 5 min followed by brief destaining. Rnt1 protein was electroeluted from gel slices in 0.1% SDS, 37.5 mM Tris-HCl, pH 8.8, and dialyzed to 0.9% saline, then used as antigen for subcutaneous immunization of a New Zealand White rabbit. Initial immunization was prepared by mixing 200–400 mg of Rnt1p with an equal volume of Freund's Complete Adjuvant. Boost immunizations were at 3–4 weekly intervals using protein purified as described and prepared for immunization with an equal volume of Freund's Incomplete Adjuvant. Crude sera containing Rnt1p antibodies was diluted 1:10,000 and used as primary polyclonal Rnt1p antibodies in western immunoblot assays according to standard protocols.

Yeast *RNT1* mutations

The *RNT1* gene as a *Bam*HI-*Xho*I fragment in the *LEU2* plasmid pRS315 (pRS315-*RNT1*) was modified by oligonucleotide mutagenesis to place an *Nde*I site at the start codon, creating pRS315-*RNT1-Nde*I. The *RNT1*Δ2–198 allele was constructed by subcloning the *Nde*I-*Bcl*I fragment from pΔ2–198 into pRS315-*RNT1*-Nde digested with *Nde*I and *Bcl*I, pRS315-*RNT1*Δ395–427 was produced by *Pst*I restriction digest and religation of pRS315-*RNT1*-Nde.

To create temperature-sensitive mutations, a fragment spanning the open reading frame of *RNT1* was amplified by mutagenic PCR (Cadwell & Joyce, 1992). The PCR product was cotransformed into the *rnt1::HIS3* knockout strain 44-0 carrying pRS316-*RNT1*, along with a gapped linear fragment of pRS315-*RNT1* produced by *Avr*II cleavage. Strain 44-0 was constructed by replacing the wild-type allele with the *rnt1::HIS3* allele created by replacing the *Avr*II fragment spanning most of the *RNT1* coding sequences with the 1.8-kb *HIS3 Bam*HI fragment (Abou Elela & Ares, 1998). After selection on plates lacking leucine, transformants were replica plated onto 5-FOA to select for cells that had lost the URA3 plasmid. Colonies that grew on 5-FOA at 26 °C were replica plated to 30 °C and 37 °C to screen for temperature sensitivity. Plasmid DNA was recovered from strains that showed a temperature-sensitive phenotype, retested, and sequenced to identify mutations. Allele *rnt1-47* contains a single substitution I338T. Allele *rnt1-53* contained the following substitutions: N20D, N237S, and F298S.

RNT1 function in vivo

RNT1 plasmids were transformed into the *rnt1::HIS3* knockout strain, streaked on SCD-leu, and incubated at 26 °C and at 37 °C. For RNA analysis, strains were grown in SCD-leucine liquid media at 26 °C to an OD of 1.0 and total RNA was extracted as described previously (Ares & Igel, 1990). Temperature-sensitive strain *rnt1*-47 was grown to an OD of 0.6, then shifted to nonpermissive temperature for 24 h before RNA extraction. The extent of formation of 25S RNA 3′ ends was assayed by ribonuclease protection as previously described (Abou Elela et al., 1996), with modification. Briefly,

100,000 cpm of an antisense transcript containing 175 nt of 25S ribosomal RNA and 284 nt downstream of the mature 25S 3′ end were hybridized for 12 h at 42 °C with 10 μg of total RNA in 80% formamide buffer. RNA hybrids were digested for 30 min at 30 °C with 0.067 Kuniz units/μL of RNase A in 400 mM NaCl. Protected RNA was extracted with phenol/chloroform, ethanol precipitated, and analyzed on 6% polyacrylamide gels.

ACKNOWLEDGMENTS

We thank Rhonda Perriman for valuable discussions, contributions, and critical reading of this manuscript; Haller Igel for technical assistance and help; and members of the Ares Laboratory for advice. We would also like to thank G. Chanfreau and S. Abou Elela for communication of results prior to publication. This work was supported by Grant GM 55557 from the National Institute of General Medical Sciences to M.A.

Received February 28, 2000; returned for revision March 15, 2000; revised manuscript received May 6, 2000

REFERENCES

Abou Elela S, Ares M Jr. 1998. Depletion of yeast RNase III blocks correct U2 3′ end formation and results in polyadenylated but functional U2 snRNA. *EMBO J 17*:3738–3746.

Abou Elela SA, Igel H, Ares M Jr. 1996. RNase III cleaves eukaryotic preribosomal RNA at a U3 snoRNP-dependent site. *Cell 85*:115–124.

Allmang C, Kufel J, Chanfreau G, Mitchell P, Petfalski E, Tollervey D. 1999. Functions of the exosome in rRNA, snoRNA and snRNA synthesis. *EMBO J 18*:5399–5410.

Allmang C, Tollervey D. 1998. The role of the 3′ external transcribed spacer in yeast pre-rRNA processing. *J Mol Biol 278*:67–78.

Ares M, Igel H. 1990. Lethal and temperature-sensitive mutations and their suppressors identify an essential structural element in U2 small nuclear RNA. *Genes & Dev 4*:2132–2145.

Bevilacqua PC, George CX, Samuel CE, Cech TR. 1998. Binding of the protein kinase PKR to RNAs with secondary structure defects: Role of the tandem A-G mismatch and noncontiguous helixes. *Biochemistry 37*:6303–6316.

Cadwell RC, Joyce GF. 1992. Randomization of genes by PCR mutagenesis. *PCR Methods Appl 2*:28–33.

Chanfreau G, Buckle M, Jacquier A. 2000. Recognition of a conserved class of RNA tetraloops by *Saccharomyces cerevisiae* RNase III. *Proc Natl Acad Sci USA 97*:3142–3147.

Chanfreau G, Elela SA, Ares M Jr, Guthrie C. 1997. Alternative 3′-end processing of U5 snRNA by RNase III. *Genes & Dev 11*: 2741–2751.

Chanfreau G, Legrain P, Jacquier A. 1998a. Yeast RNase III as a key processing enzyme in small nucleolar RNAs metabolism. *J Mol Biol 284*:975–988.

Chanfreau G, Rotondo G, Legrain P, Jacquier A. 1998b. Processing of a dicistronic small nucleolar RNA precursor by the RNA endonuclease Rnt1. *EMBO J 17*:3726–3737.

Conrad C, Rauhut R, Klug G. 1998. Different cleavage specificities of RNases III from *Rhodobacter capsulatus* and *Escherichia coli*. *Nucleic Acids Res 26*:4446–4453.

Hughes JM, Ares M Jr. 1991. Depletion of U3 small nucleolar RNA inhibits cleavage in the 5′ external transcribed spacer of yeast pre-ribosomal RNA and impairs formation of 18S ribosomal RNA. *EMBO J 10*:4231–4239.

Jucker FM, Pardi A. 1995. GNRA tetraloops make a U-turn. *RNA 1*:219–222.

Kufel J, Dichtl B, Tollervey D. 1999. Yeast Rnt1p is required for cleavage of the pre-ribosomal RNA in the 3′ ETS but not the 5′ ETS. *RNA 5*:909–917.

Lamontagne B, Tremblay A, Abou Elela S. 2000. The N-terminal domain that distinguishes yeast from bacterial RNase III contains a dimerization signal required for efficient double-stranded RNA cleavage. *Mol Cell Biol 20*:1104–1115.

Lehmann KA, Bass BL. 1999. The importance of internal loops within RNA substrates of ADAR1. *J Mol Biol 291*:1–13.

Li HD, Zagorski J, Fournier MJ. 1990. Depletion of U14 small nuclear RNA (snR128) disrupts production of 18S rRNA in *Saccharomyces cerevisiae*. *Mol Cell Biol 10*:1145–1152.

Milligan JF, Uhlenbeck OC. 1989. Synthesis of small RNAs using T7 RNA polymerase. *Methods Enzymol 180*:51–62.

Nagel RJ, Lancaster AM, Zahler AM. 1998. Specific binding of an exonic splicing enhancer by the pre-mRNA splicing factor SRp55. *RNA 4*:11–23.

Nicholson AW. 1999. Function, mechanism and regulation of bacterial ribonucleases. *FEMS Microbiol Rev 23*:371–390.

Qu LH, Henras A, Lu YJ, Zhou H, Zhou WX, Zhu YQ, Zhao J, Henry Y, Caizergues-Ferrer M, Bachellerie JP. 1999. Seven novel methylation guide small nucleolar RNAs are processed from a common polycistronic transcript by Rat1p and RNase III in yeast. *Mol Cell Biol 19*:1144–1158.

Ramos A, Grunert S, Adams J, Micklem DR, Proctor MR, Freund S, Bycroft M, St Johnston D, Varani G. 2000. RNA recognition by a Staufen double-stranded RNA-binding domain. *EMBO J 19*:997–1009.

Rotondo G, Frendewey D. 1996. Purification and characterization of the Pac1 ribonuclease of *Schizosaccharomyces pombe*. *Nucleic Acids Res 24*:2377–2386.

Rotondo G, Gillespie M, Frendewey D. 1995. Rescue of the fission yeast snRNA synthesis mutant snm1 by overexpression of the double-strand-specific Pac1 ribonuclease. *Mol Gen Genet 247*: 698–708.

Rotondo G, Huang JY, Frendewey D. 1997. Substrate structure requirements of the Pac1 ribonuclease from *Schizosaccharmyces pombe*. *RNA 3*:1182–1193.

Ryter JM, Schultz SC. 1998. Molecular basis of double-stranded RNA–protein interactions: Structure of a dsRNA-binding domain complexed with dsRNA. *EMBO J 17*:7505–7513.

Samarsky DA, Fournier MJ. 1999. A comprehensive database for the small nucleolar RNAs from *Saccharomyces cerevisiae*. *Nucleic Acids Res 27*:161–164.

Seipelt RL, Zheng B, Asuru A, Rymond BC. 1999. U1 snRNA is cleaved by RNase III and processed through an Sm site-dependent pathway. *Nucleic Acids Res 27*:587–595.

St Johnston D, Brown NH, Gall JG, Jantsch M. 1992. A conserved double-stranded RNA-binding domain. *Proc Natl Acad Sci USA 89*:10979–10983.

Studier FW, Rosenberg AH, Dunn JJ, Dubendorff JW. 1990. Use of T7 RNA polymerase to direct expression of cloned genes. *Methods Enzymol 185*:60–89.

Zhang K, Nicholson AW. 1997. Regulation of ribonuclease III processing by double-helical sequence antideterminants. *Proc Natl Acad Sci USA 94*:13437–13441.

Zhou D, Frendewey D, Lobo Ruppert SM. 1999. Pac1p, an RNase III homolog, is required for formation of the 3′ end of U2 snRNA in *Schizosaccharomyces pombe*. *RNA 5*:1083–1098.